PERGAMON

International Journal of Solids and Structures 36 (1999) 619–637

INTERNATIONAL JOURNAL OF SOLIDS and STRUCTURES

Interaction between coplanar elliptic cracks—II shear loading

T. K. Saha[a], M. Chatterjee[b], A. Roy[a,*]

[a]*Department of Applied Mathematics, University of Calcutta, 92 A.P.C. Road, Calcutta 700 009, India*
[b]*Centre for Atmospheric Science, University of Calcutta, 92 A.P.C. Road, Calcutta 700 009, India*

Received 24 April 1997; in revised form 23 December 1997

Abstract

The present paper extends the method of integral equation developed in Part I (Roy and Chatterjee, 1994) to the three-dimensional problem of interaction between two equal coplanar elliptical cracks embedded in an infinite isotropic elastic medium under shear loading. The dual integral equations obtained from the mixed boundary value problem in the present situation are coupled and reduced to infinite systems of Fredholm integral equations of the second kind—four systems corresponding to the first crack and four to the second crack. Analytical expressions for the two tangential displacement functions have been given up to the order β^5 (β being the crack separation parameter). Numerical results for the two shear stress intensity factors, $K_2(\varphi)$ and $K_3(\varphi)$, together with the interaction effects have been tabulated and illustrated graphically.

1. Introduction

Most of the structures (e.g. nuclear reactors, pressure vessels, etc.) contain cracks developed during the manufacturing process, fabrication or service period which experiences combined mode of crack-surface displacements due to the complex mode of loading conditions. Pure mode II is experienced by shear webs in aircraft structures (see e.g. Toor, 1975). The mechanism of the "after-shock" phenomenon of an earthquake can be well explained by investigating the stress distribution due to an elliptical crack under shear (see e.g. Kostorov and Das, 1984). Thus, the problem of cracks in a pure shear elastic field is of considerable interest. But, the majority of theoretical and numerical linear elastic fracture mechanics investigations have been carried out under tension loading conditions in both two and three dimensions—possibly due to simplicity in the associated mathematics. Whatever theoretical studies exist in the literature regarding cracks under shear loading—they are mostly limited to isolated crack configurations (see e.g. Kassir and Sih, 1975;

* Author to whom correspondence should be addressed. Fax: 91332413222. E-mail: tksaha@cucc.ernet.in.

0020-7683/99/$ - see front matter
PII: S0020-7683(98)00026-2

Krenk, 1979; Martin, 1986; Nishioka and Atluri, 1983; Segedin, 1951; Smith and Sorensen, 1974).

Any material body contains a system of cracks rather than an isolated one which interact to form major cracks leading to fracture. The only analytical works, about which the authors are aware regarding interaction of the three-dimensional cracks under shear loading, are those of Fu and Keer (1969) and Kachanov and Laures (1989). Both the solutions are limited to circular cracks. Fu and Keer (1969) did neither discuss the interaction effects nor evaluated the stress intensity factors which are of physical interest. Kachanov and Laures (1989) computed some numerical results for the stress intensity factors for closely spaced penny shaped cracks under both normal and shear loadings. But, in reality, flaws in three-dimensional structural components may be fitted more accurately by elliptical cracks which can also take into account various crack shapes. In practice, this is often done in pressure vessels or aircraft attachment lugs (see e.g. *ASME*, *Boiler and Pressure Vessel Code*, 1977).

Although different numerical methods (e.g. finite element method, finite element alternating method or body force method) may calculate the stress intensity factors, the authors are unaware of any analytical solution of interacting elliptical cracks under shear loading. Thus, the present study is perhaps the first attempt in this direction. The analytical technique of Part I of this paper has been extended to solve the problem. The mathematics has not been elaborated here for simplicity. For details one may refer to Part I. The interesting features of the analytical solutions and the physically important stress intensity factors and stress magnification factors are discussed with illustrations. As it will be seen that the usual definition of stress magnification factor

$$M_i = \frac{K_i}{K_i^0} \quad (i = 2, 3),$$

where K_i is the concerned stress intensity factor and K_i^0 is that of an isolated crack, is not applicable in the present case, due to the vanishing of K_i^0 at certain crack-front points, a new quantity, the resultant stress magnification factor M^* has been defined here as

$$M^*(\varphi) = \frac{[K_2^2(\varphi) + K_3^2(\varphi)]^{1/2}}{[K_2^{0^2}(\varphi) + K_3^{0^2}(\varphi)]^{1/2}} \tag{1.1}$$

where $K_2(\varphi)$ is the shear stress intensity factor along the outward drawn normal to the crack-front point φ and $K_3(\varphi)$ is that along the tangent at φ, and $K_2^0(\varphi)$ and $K_3^0(\varphi)$ represents the same, respectively, for an isolated elliptical crack. Analytical solutions for the tangential displacement potentials are given up to the fifth order of the crack separation parameter β $(=(a/f)$, "a" being the semi-major axis of an elliptical crack and "f" being the distance between the centres of the two coplanar elliptical cracks) for constant shear loading "p" at an arbitrary direction χ to the x-axis. The interaction effect for various crack shapes and separations have been illustrated graphically. The effect of change in direction of the prescribed loading on the two cracks have been illustrated for the two cases—(i) constant shear loading in the same direction on both the cracks; and (ii) constant shear loading in opposite directions on the two cracks. For testing our results, the limiting case $f \to \infty$ has been deduced, which corresponds to the stress intensity factors for an isolated elliptic crack and agrees with corresponding results given by Kassir and Sih (1975). In this

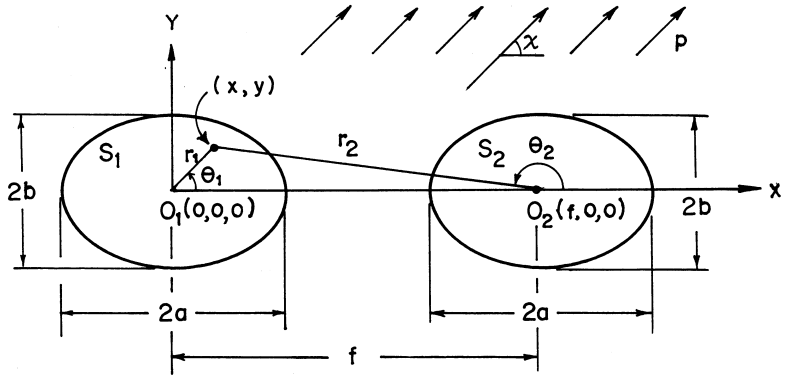

Fig. 1. Geometry of a pair of equal, coplanar elliptic cracks along with the local coordinate systems used.

case again the limiting case $(b/a) = 1$ has been deduced, which corresponds to stress intensity factors for an isolated circular crack.

The present interaction results have been compared with those presented by Kachanov and Laures (1989) for the limiting case $(b/a) = 1$ and are found to agree well for moderately and widely spaced cracks. While comparing the present results with those presented in Table 4 of Kachanov and Laures (1989) it is found that the difference in the results increases abruptly if the crack-tip spacing decreases to one-tenth of the crack radius. We don't claim that our results are accurate for such close interaction, but for completion of the figures they have been plotted together with other results.

2. Formulation of the problem

Consider two equal, coplanar elliptical cracks embedded in an infinite isotropic homogeneous elastic medium with major axes collinear and occupying the regions (see Fig. 1)

$$S_1: \quad \frac{x^2}{a^2}+\frac{y^2}{b^2} \leqslant 1; \quad z = 0,$$

$$S_2: \quad \frac{(x-f)^2}{a^2}+\frac{y^2}{b^2} \leqslant 1; \quad z = 0. \tag{2.1}$$

For crack surfaces loaded with arbitrary shear traction in an arbitrary direction, symmetry enables one to consider the equivalent half-space problem in $z \geqslant 0$ which then reduces to the problem of solving the Lamé equation of elastostatic equilibrium

$$(\lambda+\mu)\,\mathrm{grad}\,\mathrm{div}\,\underline{u}+\mu\nabla^2\underline{u} = 0 \tag{2.2}$$

subjected to the following mixed conditions on the surface $z = 0$:

$$\tau_{zz}(x,y,0) = 0 \quad \forall x,y$$
$$\tau_{zx}(x,y,0) = -\sigma_x^{(j)}(x,y) \quad \forall x,y \in S_j$$
$$\tau_{zy}(x,y,0) = -\sigma_y^{(j)}(x,y) \quad \forall x,y \in S_j \tag{2.3}$$

and,

$$u_x^{(j)}(x,y,0) = u_y^{(j)}(x,y,0) = 0 \quad \forall x,y \notin S_j$$

where $j = 1$ for the elliptical crack S_1 and $j = 2$ for S_2. The last boundary condition arises due to symmetry of the problem. $\underline{u}$ in (2.2) represents the displacement vector $\underline{u} = (u_x, u_y, u_z)$, $\sigma_x^{(j)}$ and $\sigma_y^{(j)}$ are the x and y components of the prescribed shear traction, and other symbols have their usual meaning.

An appropriate solution of $\underline{u}$ for the present problem, can be obtained in terms of two harmonic potentials $\phi(x,y,z)$ and $\psi(x,y,z)$ as

$$\underline{u} = \nabla\phi + \frac{z}{2(1-\nu)}\nabla\left(\frac{\partial\phi}{\partial z}\right) - \frac{3-4\nu}{2(1-\nu)}\frac{\partial\phi}{\partial z}\underline{e}_z + \nabla\times(\underline{e}_z\psi) \tag{2.4}$$

where ν is the Poisson's ratio and $\underline{e}_z$ is a unit vector in the z direction.

Seeking solutions of $\phi(x,y,z)$ and $\psi(x,y,z)$ as

$$[\phi(x,y,z), \psi(x,y,z)] = \frac{1}{2\pi}\int_{-\infty}^{\infty}\int_{-\infty}^{\infty}[P(\xi,\eta), Q(\xi,\eta)]\exp[i(\xi x+\eta y)-\lambda_0 z]\,\mathrm{d}\xi\,\mathrm{d}\eta \tag{2.5}$$

where $\lambda_0 = (\xi^2+\eta^2)^{1/2}$, one can show that the mixed boundary conditions are satisfied if the tangential crack-face displacements $u_x^{(j)}(x,y)$ and $u_y^{(j)}(x,y)$ satisfy the following coupled dual integral equations:

$$\sum_{j=1}^{2}\int_{-\infty}^{\infty}\int_{-\infty}^{\infty}\iint_{S_j}\lambda_0^{-1}\begin{pmatrix}\xi^2+(1-\nu)\eta^2 & \nu\xi\eta \\ \nu\xi\eta & (1-\nu)\xi^2+\eta^2\end{pmatrix}\begin{pmatrix}u_x^{(j)} \\ u_y^{(j)}\end{pmatrix}$$
$$\times\exp[i\{\xi(x-x')+\eta(y-y')\}]\,\mathrm{d}x'\,\mathrm{d}y'\,\mathrm{d}\xi\,\mathrm{d}\eta$$
$$= \frac{4\pi^2(1-\nu)}{\mu}\begin{pmatrix}\sigma_x^{(k)}(x,y) \\ \sigma_y^{(k)}(x,y)\end{pmatrix}, \quad \forall x,y \in S_k \quad (k = 1,2). \tag{2.6}$$

3. Reduction of the coupled dual integral equations

For reducing the system of coupled dual integral equations, one transforms to the polar co-ordinate system via suitable transformations mentioned in Part I. The elliptic domains are transformed to circular domains. A point P of the domain is related to the two local co-ordinate systems centred at the origins of the both ellipses by the summation theorem of Bessel functions. The unknown displacement and known stress components are expanded in Fourier series of sines and cosines. After necessary manipulations, the coefficients of sines and cosines are equated from both

sides to obtain a set of four infinite systems of integral equations (two for the sine terms and two for the cosine terms). Such a set is obtained for both cracks.

A further reduction of the two sets of integral equations to Fredholm integral equations of the second kind is performed by relating the Fourier components of tangential displacements to new entities by appropriate Abelian transformations and using standard results involving Bessel functions (see e.g. Part I).

The final form of the Fredholm integral equations of the second kind for the two sets of equations are written below:

$\forall s = 0, 1, 2, \ldots, \infty$, $(n+s)$ is even; for each s, $(n+p)$ even; $\xi, r \in [0,1]$

$$\begin{pmatrix}\Gamma^{(i)}_{s,s}(\xi)\\ \Lambda^{(i)}_{s,s}(\xi)\end{pmatrix} + \sum_{\substack{n=0\\ n\neq s}}^{\infty} \begin{pmatrix}\langle L_{n,s}(\xi,t)\Gamma^{(i)}_{n,s}(t)\rangle\\ \langle L_{n,s}(\xi,t)\Lambda^{(i)}_{n,s}(t)\rangle\end{pmatrix} = (-1)^{i+1}\begin{pmatrix}F^{(i)}_{s}(\xi)\\ G^{(i)}_{s}(\xi)\end{pmatrix} - e_s \sum_{n=0}^{\infty}\sum_{p=0}^{\infty}(-1)^n \begin{pmatrix}\langle \mathscr{K}_{s,n,p}(\xi,t)\Gamma^{(3-i)}_{n,p}(t)\rangle\\ \langle \mathscr{K}_{s,n,p}(\xi,t)\Lambda^{(3-i)}_{n,p}(t)\rangle\end{pmatrix}, \quad i = 1,2 \tag{3.1}$$

where

$$\langle A_{n,s}(t)\rangle = \int_0^1 A_{n,s}(t)\,\mathrm{d}t \tag{3.2}$$

$$\Gamma^{(j)}_{n,s}(t) = \varepsilon_s \begin{pmatrix} I^{c}_{n,s}(A,B)\Psi^{(j)}(t) + I^{sc}_{n,s}\bar{\Theta}^{(j)}_{n}(t)\\ I^{s}_{n,s}(A,B)\bar{\Psi}^{(j)}(t) + I^{cs}_{n,s}\Theta^{(j)}_{n}(t)\end{pmatrix} \tag{3.3}$$

$$\Lambda^{(j)}_{n,s}(t) = \varepsilon_s \begin{pmatrix} I^{sc}_{n,s}\bar{\Psi}^{(j)}_{n}(t) + I^{c}_{n,s}(C,D)\Theta^{(j)}_{n}(t)\\ I^{cs}_{n,s}\Psi^{(j)}_{n}(t) + I^{s}_{n,s}(C,D)\bar{\Theta}^{(j)}_{n}(t)\end{pmatrix} \tag{3.4}$$

$$\begin{pmatrix}I^{c}_{n,s}(L,M)\\ I^{s}_{n,s}(L,M)\end{pmatrix} = \frac{1}{2} i^s (-i)^n \int_0^{2\pi} \frac{L + M\cos 2X}{\Delta(k_0)} \begin{pmatrix}\cos nX \cos sX\\ \sin nX \sin sX\end{pmatrix} \mathrm{d}X \tag{3.5}$$

$$\begin{pmatrix}I^{sc}_{n,s}\\ I^{cs}_{n,s}\end{pmatrix} = \frac{1}{2} i^s (-i)^n k_0' v \int_0^{2\pi} \frac{\sin 2X}{\Delta(k_0)} \begin{pmatrix}\sin nX \cos sX\\ \cos nX \sin sX\end{pmatrix} \mathrm{d}X \tag{3.6}$$

$(L, M) = (A, B)$ or (C, D) where

$$A = 2 - \nu - k_0^2, \quad B = \nu - k_0^2, \quad C = 2 - \nu - (1-\nu)k_0^2, \quad D = -\nu - (1-\nu)K_0^2 \tag{3.7}$$

$$k_0^2 = 1 - \frac{b^2}{a^2}, \quad k_0' = \frac{b}{a}, \quad \Delta(k_0) = (1 - k_0^2 \cos^2 X)^{1/2} \tag{3.8}$$

$$\varepsilon_s = \begin{cases} 1, & s = 0\\ 2, & s > 0\end{cases}; \quad e_s = \tfrac{1}{2}\varepsilon_s \tag{3.9}$$

$$L_{n,s}(\xi,t) = (\xi t)^{1/2}\int_0^\infty kJ_{n+(1/2)}(kt)J_{s+(1/2)}(k\xi)\,\mathrm{d}k \tag{3.10}$$

$$F_s^{(i)}(\xi) = c_0\xi^{-s}\int_0^\xi \frac{r^{s+1}}{(\xi^2-r^2)^{1/2}}\begin{pmatrix}p_s^{(i)}(r)\\ \bar{p}_s^{(i)}(r)\end{pmatrix}\mathrm{d}r \tag{3.11}$$

$$G_s^{(i)}(\xi) = c_0\xi^{-s}\int_0^\xi \frac{r^{s+1}}{(\xi^2-r^2)^{1/2}}\begin{pmatrix}q_s^{(i)}(r)\\ \bar{q}_s^{(i)}(r)\end{pmatrix}\mathrm{d}r \tag{3.12}$$

$$c_0 = \frac{2\pi(1-\nu)b}{\mu}\mathscr{K}_{s,n,p}(\xi,t) = \begin{pmatrix}K_{s,n,p}(\xi,t) & 0\\ 0 & -N_{s,n,p}(\xi,t)\end{pmatrix} \tag{3.13}$$

where

$$\begin{pmatrix}K_{s,n,p}(\xi,t)\\ N_{s,n,p}(\xi,t)\end{pmatrix} = M^s_{n,p+s}(\xi,t)\pm(-1)^s M^s_{n,p-s}(\xi,t) \tag{3.14}$$

and

$$M^s_{n,p\pm s}(\xi,t) = (\xi t)^{1/2}\int_0^\infty kJ_{n+(1/2)}(kt)J_{s+(1/2)}(k\xi)J_{p\pm s}(kd_0)\,\mathrm{d}k \tag{3.15}$$

where $d_0 = (f/a)$.

Here $\Psi_n^{(j)}$, $\bar{\Psi}_n^{(j)}$ are the quantities which are related to the Fourier cosine and sine components of the displacement component $u_x^{(j)}$ by Abelian transformation. Similarly $\Theta_n^{(j)}$, $\bar{\Theta}_n^{(j)}$ correspond to $u_y^{(j)}$. Also $p_s^{(j)}$, $\bar{p}_s^{(j)}$ are Fourier cosine and sine components corresponding to the x-component $\sigma_x^{(j)}$ of the prescribed traction and $q_s^{(j)}$, $\bar{q}_s^{(j)}$ are similar entities for $\sigma_y^{(j)}$.

It may be noted that the double summation term in the r.h.s. of (3.1) contains the displacement functions corresponding to the neighbouring elliptic crack and, hence, contributes to the interaction effect. Also it may be noted, that this double sum contains $M^s_{n,p\pm s}(\xi,t)$ which has a closed form expression [see e.g. eqn (38) of part I] that can be expanded in a power series in β $[=(1/d_0)]$ with β^3 in the first term. Clearly, for a finite crack size

$$\lim_{d_0\to\infty} M^s_{n,p\pm s}(\xi,t) = 0.$$

Thus, the interaction effect decreases with increase in crack distance, and we get back the single crack solution as a limiting situation. In this situation, the infinite system (3.1) reduces to a single equation for the case $s = 0$, and the single sum in the l.h.s. of (3.1) is identically zero. Therefore, it may be remarked that the equations corresponding to the cases $s \geqslant 1$ together with the single sum in l.h.s. generate that part of the solution, which reflects the effect of the neighbouring crack if the double sum in the r.h.s. exists, too, for finite d_0.

4. Approximate analytical solution

The method of solution is the same perturbation technique as adopted in Part I of this paper. Once the solution for the single cracks are obtained, that for the neighbouring crack is substituted in the r.h.s. of (3.1) resulting in a known series in β. Each term of the series corresponds to particular values of s (finite number) giving rise to a finite set of linear equations. Again, each term in powers of β is also a known polynomial in ξ. Hence the right hand side of the set of linear equations consists of polynomials in ξ, so that the left hand side must also be a polynomial of the same type in ξ. Equating powers of ξ we get the solutions for the interaction effect.

The smaller the value of β, the quicker is the convergence. For non-overlapping cracks $\beta < \frac{1}{2}$, so the series always converges theoretically. The only requirement is that for close cracks higher order terms in β will be required. Extraction of higher order terms in β requires intensive calculation, so from practical point of view, in case of close cracks one must turn to numerical solution of the integral eqns (3.1).

In the present article analytical solutions are obtained up to the order β^5 for a prescribed constant tangential loading p in an arbitrary direction χ to the x-axis. The solutions are expected to yield accurate results for moderately and widely spaced cracks.

We quote below the solutions for first crack (suppressing the superscript in the solutions) if the major axis of the cracks are collinear:

$$
\begin{aligned}
\Psi_0(\xi) &= [a_0^{(0)} + a_0^{(1)}\beta^3 + a_0^{(2)}\beta^5]\xi + [a_0^{(3)}\beta^5]\xi^3 \\
\Psi_1(\xi) &= [a_1^{(1)}\beta^4]\xi^2 \\
\bar{\Psi}_1(\xi) &= [\bar{a}_1^{(1)}\beta^4]\xi^2 \\
\Psi_2(\xi) &= [a_2^{(1)}\beta^5]\xi^3 \\
\bar{\Psi}_2(\xi) &= [\bar{a}_2^{(1)}\beta^5]\xi^3 \\
\Theta_0(\xi) &= [b_0^{(0)} + b_0^{(1)}\beta^3 + b_0^{(2)}\beta^5]\xi + [b_0^{(3)}\beta^5]\xi^3 \\
\Theta_1(\xi) &= [b_1^{(1)}\beta^4]\xi^2 \\
\bar{\Theta}_1(\xi) &= [\bar{b}_1^{(1)}\beta^4]\xi^2 \\
\Theta_2(\xi) &= [b_2^{(1)}\beta^5]\xi^3 \\
\bar{\Theta}_2(\xi) &= [\bar{b}_2^{(1)}\beta^5]\xi^3
\end{aligned}
\tag{4.1a}
$$

$$
\Psi_n(\xi), \quad \bar{\Psi}_n(\xi), \quad \Theta_n(\xi), \quad \bar{\Theta}_n(\xi) \simeq 0(\beta^6) \quad \forall n \geqslant 3. \tag{4.1b}
$$

The different symbols used in (4.1a,b) are given in Appendix A.

5. Numerical results

Recently, expressions for K_2 and K_3 at a representative point $(a\cos\varphi, b\sin\varphi)$ on the crack border were given by Roy and Chatterjee (1992), following definitions of Martin (1986), as

$$K_2(\varphi) = \frac{2\mu}{\pi(1-\nu)b}\left(\frac{b}{a}\right)^{1/2}(a^2\sin^2\varphi + b^2\cos^2\varphi)^{-1/4} \times \left[\sum_{n=0}^{\infty}(b\cos\varphi\Psi_n(1) + a\sin\varphi\Theta_n(1))\cos n\varphi + \sum_{n=1}^{\infty}(b\cos\varphi\bar{\Psi}_n(1) + a\sin\varphi\,\bar{\Theta}_n(1))\sin n\varphi\right] \quad (5.1)$$

and

$$K_3(\varphi) = \frac{2\mu}{\pi b}\left(\frac{b}{a}\right)^{1/2}(a^2\sin^2\varphi + b^2\cos^2\varphi)^{-1/4} \times \left[\sum_{n=0}^{\infty}(-a\sin\varphi\Psi_n(1) + b\cos\varphi\Theta_n(1))\cos n\varphi + \sum_{n=1}^{\infty}(-a\sin\varphi\bar{\Psi}_n(1) + b\cos\varphi\,\bar{\Theta}_n(1))\sin n\varphi\right]. \quad (5.2)$$

In the limit $f \to \infty$, the above expressions reduce to

$$K_2^0 = pk_0^2\sqrt{k_0'}(a^2\sin^2\varphi + b^2\cos^2\varphi)^{-1/4} \times \left[\frac{a\sin\chi\sin\varphi}{(k_0^2+\nu k_0'^2)E(k_0) - \nu k_0'^2K(k_0)} + \frac{b\cos\chi\cos\varphi}{(k_0^2-\nu)E(k_0) + \nu k_0'^2K(k_0)}\right] \quad (5.1a)$$

and

$$K_3^0 = pk_0^2\sqrt{k_0'}(1-\nu)(a^2\sin^2\varphi + b^2\cos^2\varphi)^{-1/4} \times \left[\frac{a\cos\chi\sin\varphi}{(\nu-k_0^2)E(k_0) - \nu k_0'^2K(k_0)} - \frac{b\sin\chi\cos\varphi}{\nu k_0'^2K(k_0) - (k_0^2+\nu k_0'^2)E(k_0)}\right]$$

$$k_0^2 = 1-\frac{b^2}{a^2}, \quad k_0' = (1-k_0^2)^{1/2} = \frac{b}{a}. \quad (5.2a)$$

These are expressions for K_2 and K_3 for an isolated elliptic crack under uniform shear loading p at an arbitrary direction χ to the x-axis given earlier by Kassir and Sih (1975, eqns 3.54a and 3.54b). In the above expressions $K(k_0)$ and $E(k_0)$ are elliptic integrals of the first and second kind, respectively.

For $(b/a) = 1$, $E(k_0) = K(k_0) = (\pi/2)$ and in that case (5.1a) and (5.2a) reduces, respectively, to

$$K_2^0 = \frac{2\sqrt{a}p}{\pi}\cos(\chi-\varphi) \quad (5.1b)$$

and

$$K_3^0 = \frac{2\sqrt{a}p(1-\nu)}{\pi}\sin(\chi-\varphi). \quad (5.2b)$$

These are the expressions for K_2 and K_3 for an isolated circular crack.

In the solutions (4.1a,b) $a_0^{(0)}\xi$ and $b_0^{(0)}\xi$ are the single crack solutions and the other terms are present due to the effect of the second crack on the first, and so necessarily contains the terms

Table 1
Two equal coplanar circular cracks under shear loading. The values of max K_2/K_2^0 ($\nu = 0.5$)

	max K_2/K_2^0		
$(f/a)-2$	Present method	Kachanov and Laures	Difference percentage
0.1	1.1203	1.3587	21.6
0.5	1.0613	1.0833	2.2
1.0	1.0309	1.0316	0.07
1.5	1.0176	1.0159	0.17
2.0	1.0109	1.0092	0.17
3.0	1.0050	1.0039	0.11
5.0	1.0016	1.0008	0.08

$p_0^{(2)}(r)$ and $q_0^{(2)}(r)$ in their expressions. The solutions (4.1a,b) are given for the case where the loading is in the same direction on both crack faces, i.e.

$$p_0^{(1)}(r) = p_0^{(2)}(r) = p\cos\chi, \quad q_0^{(1)}(r) = q_0^{(2)}(r) = p\sin\chi. \tag{5.4a}$$

But another interesting case may be considered simultaneously, where the loading is in the opposite direction on the two crack faces, i.e.

$$p_0^{(1)}(r) = -p_0^{(2)}(r) = p\cos\chi, \quad q_0^{(1)}(r) = -q_0^{(2)}(r) = p\sin\chi. \tag{5.4b}$$

In this case a negative sign will be introduced in the interaction terms due to the presence of the terms $p_0^{(2)}(r)$ and $q_0^{(2)}(r)$. Thus, it may be noted that when $M^*(\varphi)$ will be plotted against the elliptic angle φ, the case (5.4b) will produce mirror symmetry of the case (5.4a) about $M^*(\varphi) = 1.0$. This situation has been illustrated graphically.

For the case of comparison, the only results available to the authors are those of Kachanov and Laures (1989) for the limiting case $(b/a) = 1$ (i.e. for coplanar circular cracks) where the cracks are strongly interacting. It may be noted that the present definitions of K_2 and K_3 differs from those of Kachanov and Laures (1989) by a factor of $\sqrt{2}$.

In the present article no attempt has been made to compare results of very close interactions. For such interactions higher order terms in β are necessary in the solutions (4.1a,b). Also, the method of Kachanov and Laures (1989) is only an approximate one and not exact. Hence their solution requires further verification.

In Table 1 the comparison has been performed for the maximum value of $M_2(\varphi)$ with the results given in Table 4 of Kachanov and Laures (1989) for $\nu = 0.5$. The present results are seen to conform with theirs for moderately and widely spaced cracks. When the spacing

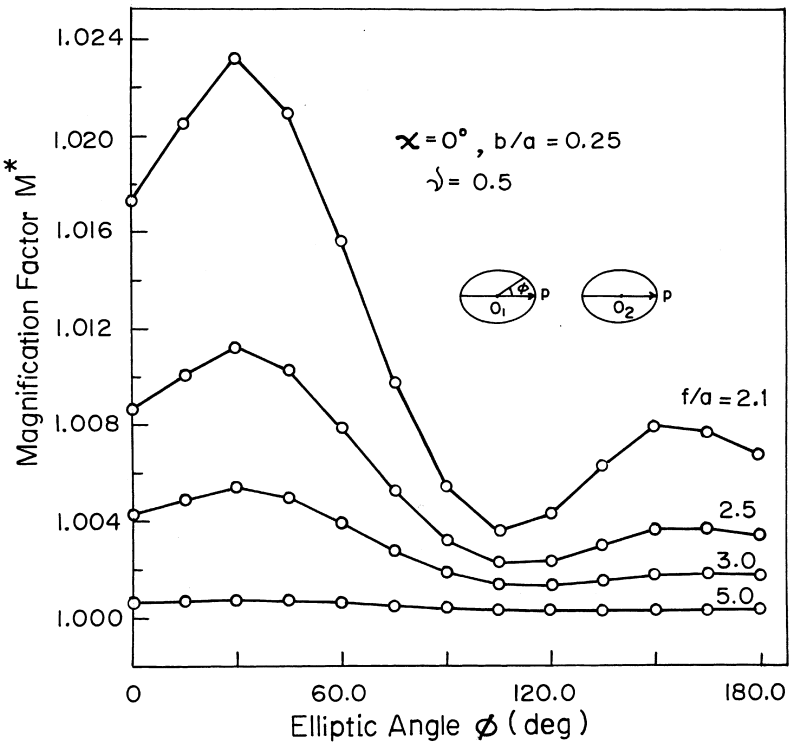

Fig. 2. Variation of resultant stress magnification factor $M^*(\phi)$ with elliptic angle ϕ for various crack separations $(f/a) = 2.1, 2.5, 3.0, 5.0$ when the shear stress is applied at $\chi = 0^\circ$ on both the cracks of aspect ratio 0.25. $v = 0.5$.

$(d_0-2) = 0.5$, the difference in the two results is 2.2% and when it is 0.1 the difference increases to 21.5%. In the last case their result seems to be an overestimation of the exact result.

Figures 2 and 3 illustrate the variation of $M^*(\varphi)$ with φ for cracks with $(b/a) = 0.25$ at various spacings. These figures illustrate the case (5.4a) : for $\chi = 60^\circ$, Fig. 3 reveals that $M^*(\varphi)$ is a mixture of amplification and shielding. Maximum shielding is attained at $\varphi = 300^\circ$ and is about 1.81% for $(d_0-2) = 0.1$ and 0.81% for $(d_0-2) = 0.5$.

Figures 4 and 5 illustrates the case (5.4b) for the same crack shape and spacings as in Figs 2 and 3. The mirror symmetry of the Figs 2 and 3 about $M^* = 1.0$ is observed in this case as mentioned earlier.

Figure 6 illustrates the variation of $M^*(\varphi)$ with φ for different χ (case 5.4a) at $(d_0-2) = 0.5$ with $(b/a) = 0.25$.

Figures 7 and 8 shows variations in $M^*(\varphi)$ with change in b/a (case 5.4a). Narrower the crack, larger is the region of shielding. For $(b/a) = 0.125$ maximum shielding is about 2.2% attained at $\varphi = 300^\circ$ and for $(b/a) = 0.75$ it is only about 0.03%.

Table 2 shows the values of maximum and minimum $M^*(\varphi)$ for different values of χ and b/a when $(d_0-2) = 0.5$. The values within the parenthesis are the angles where these are attained.

Figures 9 and 10 illustrates the dependence of $M^*(\varphi)$ on v. Figure 9 gives illustrations for $\chi = 0^\circ$ and Fig. 10 gives those for $\chi = 60^\circ$. Clearly, increase in v increases the effect of interaction.

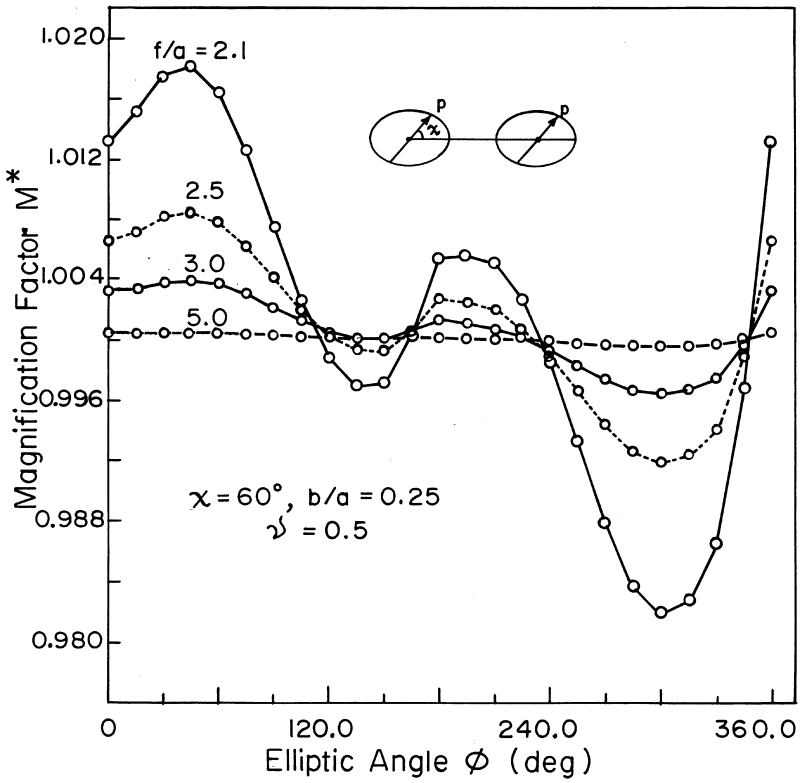

Fig. 3. Same as Fig. 2, except that now the shear is applied at an angle $\chi = 60^\circ$ on both the cracks.

6. Conclusions

An analytical solution to the problem of interaction between two coplanar elliptical cracks under uniform shear loading at arbitrary direction has been obtained following the method of solution in Part I of this paper. The solutions are expected to be accurate for moderate and weak interactions.

In the limiting case $f \to \infty$, the stress intensity factors for isolated elliptic cracks under shear loading were rederived. Also, in this case the results for the limiting case $(b/a) = 1$ were obtained which gives results for isolated circular cracks under shear loading.

For moderate and wide spacings of the cracks, the results for the limiting case of $(b/a) = 1$ were compared with those given by Kachanov and Laures (1989) and found to be conformable.

The present solutions are expected to help structural engineers and material scientists to encounter more realistic situations of interactions under complex loading conditions.

Here solutions are given for moderately and weakly interacting coplanar elliptic cracks of equal sizes when the major axis are collinear. Other interesting situations, where macrocracks interacts with coplanar microcracks, be it penny shaped or elliptical, and positioned in arbitrary directions, are under consideration and are expected to be reported in later publications.

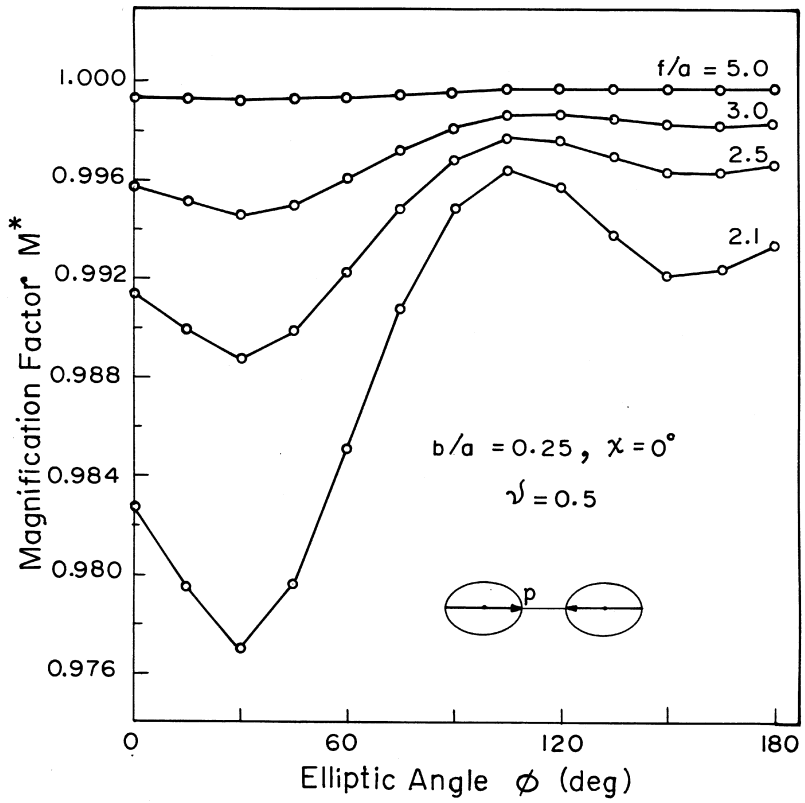

Fig. 4. Variation of resultant stress magnification factor $M^*(\phi)$ with elliptic angle ϕ for same crack separations and aspect ratio as in Fig. 2 with the tangential loading now being applied at $\chi = 0^\circ$ on S_1 and at $\chi = 180^\circ$ on S_2. $\nu = 0.5$.

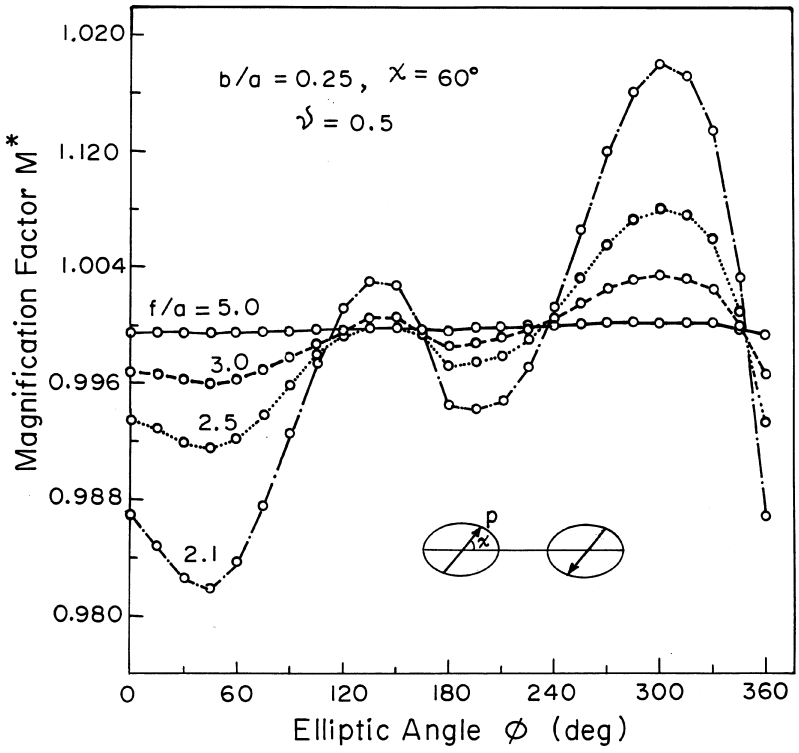

Fig. 5. Same as Fig. 4 but the loading now acts along $\chi = 60^\circ$ on S_1 and $\chi = 240^\circ$ on S_2.

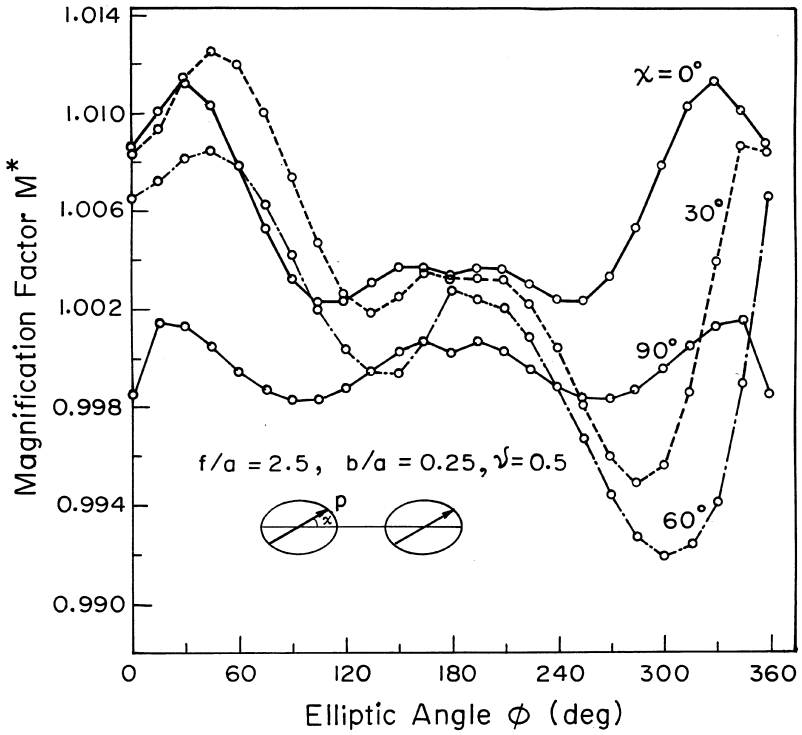

Fig. 6. Variation of $M^*(\phi)$ with elliptic angle ϕ for various loading angles χ (same on both the cracks) when $(f/a) = 2.5$ and aspect ratio of the cracks is 0.25. $\nu = 0.5$.

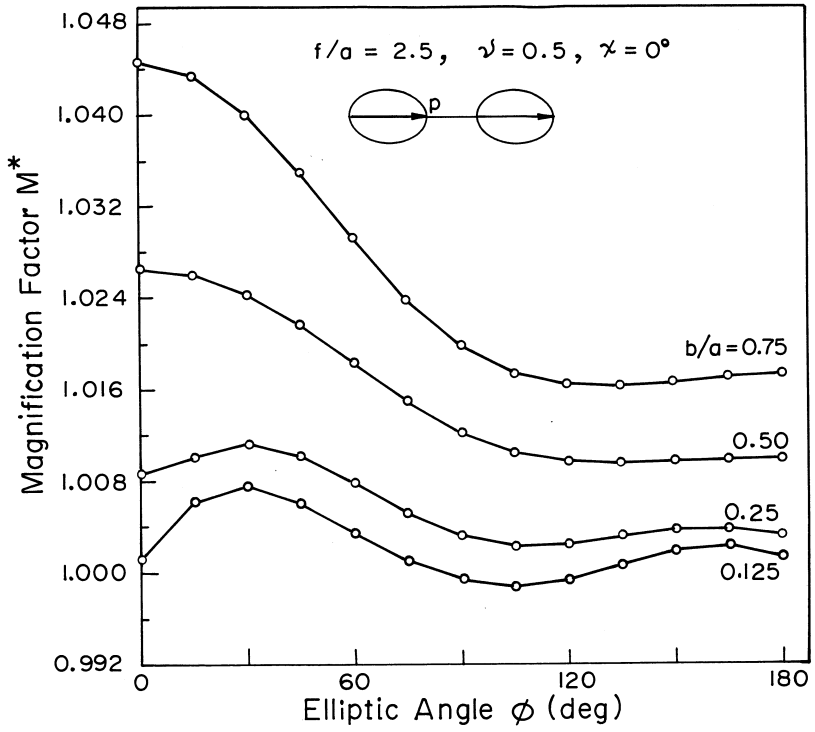

Fig. 7. Variation of $M^*(\phi)$ with ϕ for various aspect ratios (0.75, 0.5, 0.25, 0.125) when tangential loading angle $\chi = 0^\circ$ on both the cracks and $(f/a) = 2.5$. $\nu = 0.5$.

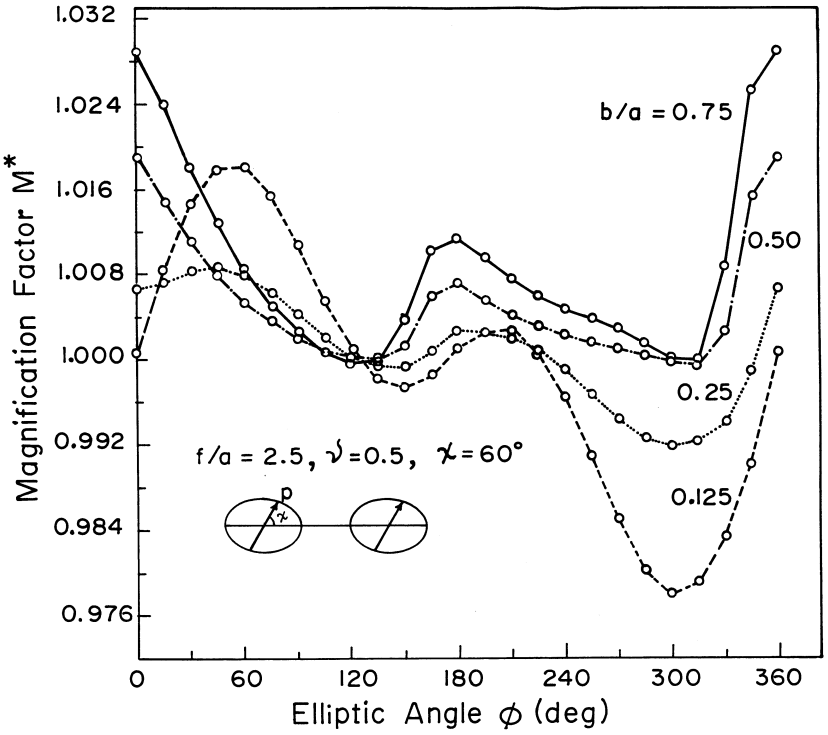

Fig. 8. Same as Fig. 7, except that now $\chi = 60^\circ$ on both the cracks.

Table 2
Two equal coplanar elliptical cracks of variable aspect ratio situated at a distance of $0.5a$ apart. The values of maximum and minimum resultant Stress Magnification factor M^* for different loading angles. [$v = 0.5$, $(f/a) = 2.5$]

	Max $M^*(\phi)$				Min $M^*(\phi)$			
b/a $\chi\rightarrow$	0°	30°	60°	90°	0°	30°	60°	90°
0.75	1.04466 (0°)	1.04508 (345°)	1.02874 (0°)	1.00129 (45°, 315°)	1.01629 (135°, 225°)	1.00928 (105°)	0.99974 (120°)	0.99992 (0°)
0.5	1.02657 (0°)	1.02781 (345°)	1.01901 (0°)	1.00074 (30°, 330°)	1.00954 (135°, 225°)	1.00579 (255°)	0.99952 (315°)	0.99957 (0°)
0.25	1.01128 (30°, 330°)	1.01251 (45°)	1.00851 (45°)	1.00149 (15°, 345°)	1.00228 (105°, 255°)	0.99493 (285°)	0.99190 (300°)	0.99830 (90°, 270°)
0.125	1.00759 (30°, 330°)	1.02088 (60°)	1.01808 (60°)	1.00223 (15°, 345°)	0.99879 (105°, 255°)	0.97941 (300°)	0.97804 (300°)	0.99742 (90°, 270°)

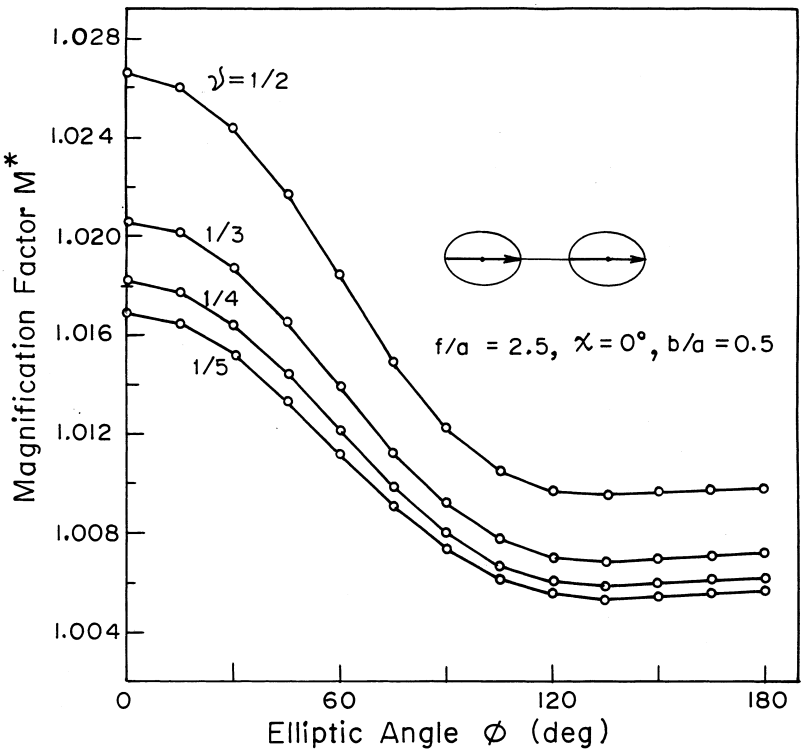

Fig. 9. Variation of $M^*(\phi)$ for various Poisson's ratio $v = \frac{1}{2}, \frac{1}{3}, \frac{1}{4}, \frac{1}{5}$ when $\chi = 0^\circ$ on both the cracks of aspect ratio 0.5 and $(f/a) = 2.5$.

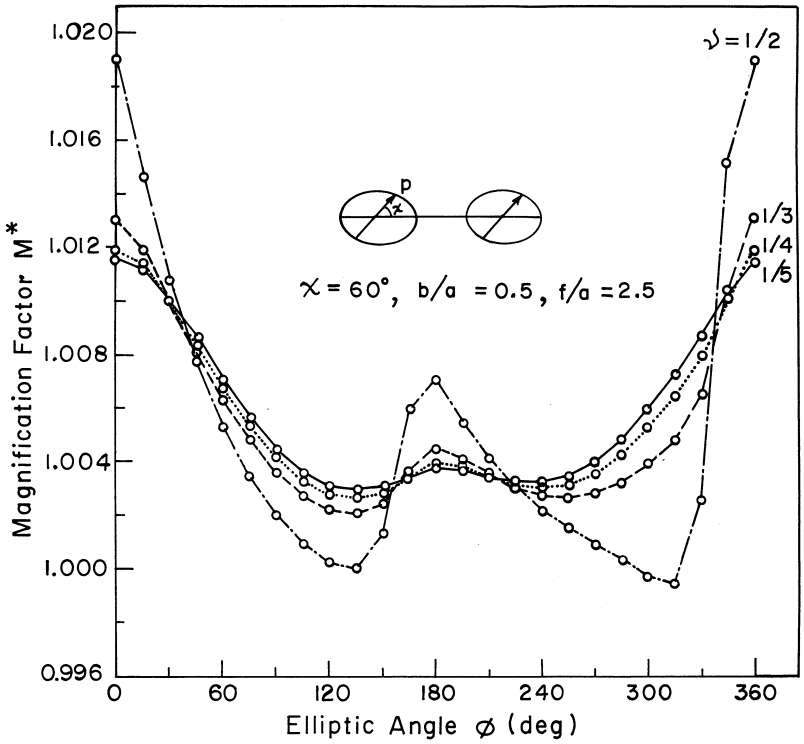

Fig. 10. Same as Fig. 9, except that now $\chi = 60^\circ$ on both the cracks.

Acknowledgements

The valuable comments of the reviewers are gratefully acknowledged.

Appendix

List of symbols used in (4.1a) and (4.1b):

$$a_0^{(0)} = \gamma$$

$$a_0^{(1)} = \frac{2\gamma}{3\pi}\frac{s_0}{I^c_{0,0}(A,B)}$$

$$a_0^{(2)} = \frac{1}{I^c_{0,0}(A,B)}\left[(3\gamma/5\pi)s_1 - \frac{3}{2}I^c_{2,0}(A,B)A_{01} - \frac{3}{2}I^{sc}_{2,0}A_{02}\right]$$

$$a_0^{(3)} = A_{03}$$

$$a_1^{(1)} = \frac{1}{\Omega_1}\left[\frac{2\gamma}{3\pi}s_0 I^s_{1,1}(C,D) + \frac{2\gamma}{9\pi}p_0 I^{sc}_{1,1}\right]$$

$$\bar{a}_1^{(1)} = -\frac{1}{\Delta_1}\left[\frac{2\lambda}{9\pi}p_0 I^c_{1,1}(C,D) + \frac{2\lambda}{3\pi}s_0 I^{cs}_{1,1}\right]$$

$$a_2^{(1)} = A_{01}$$

$$\bar{a}_2^{(1)} = B_{02}$$

$$b_0^{(0)} = \lambda$$

$$b_0^{(1)} = \frac{2\lambda}{3\pi}\frac{S_0}{I^c_{0,0}(C,D)}$$

$$b_0^{(2)} = \frac{1}{I^c_{0,0}(C,D)}\left[(3\lambda/5\pi)S_1 - \frac{3}{2}I^c_{2,0}(C,D)B_{01} - \frac{3}{2}I^{sc}_{2,0}B_{02}\right]$$

$$b_0^{(3)} = B_{03}$$

$$b_1^{(1)} = \frac{1}{\Delta_1}\left[\frac{2\lambda}{3\pi}S_0 I^s_{1,1}(A,B) + \frac{2\lambda}{9\pi}p_0 I^{sc}_{1,1}\right]$$

$$\bar{b}_1^{(1)} = -\frac{1}{\Omega_1}\left[\frac{2\gamma}{9\pi}p_0 I^c_{1,1}(A,B) + \frac{2\gamma}{3\pi}s_0 I^{cs}_{1,1}\right]$$

$$b_2^{(1)} = B_{01}$$

$$\bar{b}_2^{(1)} = A_{02}$$

where,

$$\gamma = \frac{2\pi(1-\nu)b}{\mu}\cdot\frac{p\cos\chi}{I^c_{0,0}(A,B)}$$

$$\lambda = \frac{2\pi(1-\nu)b}{\mu}\cdot\frac{p\sin\chi}{I^c_{0,0}(C,D)}$$

$$A_{01} = \frac{1}{\nabla_1}\left[\frac{2\gamma}{5\pi}s_1\Gamma_3 + \frac{2\gamma}{3\pi}s_2\Gamma_5 + \frac{16\gamma}{45\pi}p_0\Gamma_1(A,B)\right]$$

$$A_{02} = \frac{1}{\nabla_1}\left[\frac{2\gamma}{5\pi}s_1\Gamma_7(A,B) + \frac{2\gamma}{3\pi}s_2\Gamma_1(A,B) - \frac{16\gamma}{45\pi}p_0\Omega_0(A,B)\right]$$

$$A_{03} = \frac{1}{\nabla_1}\left[\frac{\gamma}{\pi}s_1\Omega_2 + \frac{5\gamma}{3\pi}s_2\Gamma_3 + \frac{8\gamma}{9\pi}p_0\Gamma_2(A,B)\right]$$

$$B_{01} = \frac{1}{\nabla_2}\left[\frac{2\lambda}{5\pi}S_1\Gamma_4 + \frac{2\lambda}{3\pi}S_2\Gamma_6 + \frac{16\lambda}{45\pi}p_0\Gamma_1(C,D)\right]$$

$$B_{02} = \frac{1}{\nabla_2}\left[\frac{2\lambda}{5\pi}S_1\Gamma_5(C,D) + \frac{2\lambda}{3\pi}S_2\Gamma_1(C,D) - \frac{16\lambda}{45\pi}p_0\Omega_0(C,D)\right]$$

$$B_{03} = \frac{1}{\nabla_2}\left[\frac{\lambda}{\pi}S_1\Omega_3 + \frac{5\lambda}{3\pi}S_2\Gamma_4 + \frac{8\lambda}{9\pi}p_0\Gamma_2(C,D)\right].$$

Here,

$$\Omega_0(L,M) = I^c_{0,0}(L,M)I^c_{2,2}(L,M) - \{I^c_{0,2}(L,M)\}^2$$

$$\Omega_1 = I^c_{1,1}(A,B)I^s_{1,1}(C,D) - (I^{sc}_{1,1})^2$$

$$\Omega_2 = I^c_{2,2}(A,B)I^s_{2,2}(C,D) - (I^{sc}_{2,2})^2$$

$$\Omega_3 = I^c_{2,2}(C,D)I^s_{2,2}(A,B) - (I^{sc}_{2,2})^2$$

$$\Delta_1 = I^c_{1,1}(C,D)I^s_{1,1}(A,B) - (I^{sc}_{1,1})^2$$

$$\nabla_1 = I^s_{2,2}(C,D)\Omega_0(A,B) + I^{sc}_{2,2}\Gamma_1(A,B) + I^{cs}_{0,2}\Gamma_2(A,B)$$

$$\nabla_2 = I^s_{2,2}(A,B)\Omega_0(C,D) + I^{sc}_{2,2}\Gamma_1(C,D) + I^{cs}_{0,2}\Gamma_2(C,D)$$

$$\Gamma_1(L,M) = I^c_{0,2}(L,M)I^{cs}_{0,2} - I^c_{0,0}(L,M)I^{cs}_{2,2}$$

$$\Gamma_2(L,M) = I^c_{0,2}(L,M)I^{cs}_{2,2} - I^c_{2,2}(L,M)I^{cs}_{0,2}$$

$$\Gamma_3 = I^c_{0,2}(A,B)I^s_{2,2}(C,D) - I^{cs}_{0,2}I^{cs}_{2,2}$$

$$\Gamma_4 = I^c_{0,2}(C,D)I^s_{2,2}(A,B) - I^{cs}_{0,2}I^{cs}_{2,2}$$

$$\Gamma_5 = I^c_{0,0}(A,B)I^s_{2,2}(C,D) - (I^{cs}_{0,2})^2$$

$$\Gamma_6 = I^c_{0,0}(C,D)I^s_{2,2}(A,B) - (I^{cs}_{0,2})^2$$

$$\Gamma_7(L,M) = I^c_{2,2}(L,M)I^{cs}_{0,2} - I^c_{0,2}(L,M)I^{cs}_{2,2}$$

$$p_0 = 4\sum_{m=1}^{\infty} m(1-4m^2)I^{cs}_{0,2m}$$

$$s_0 = I^c_{0,0}(A,B) + 2\sum_{m=1}^{\infty} I^c_{0,2m}(A,B)(1-4m^2)$$

$$S_0 = I^c_{0,0}(C,D) + 2\sum_{m=1}^{\infty} I^c_{0,2m}(C,D)(1-4m^2)$$

$$s_1 = I^c_{0,0}(A,B) + \frac{2}{9}\sum_{m=1}^{\infty} I^c_{0,2m}(A,B)(1-4m^2)(9-4m^2)$$

$$S_1 = I^c_{0,0}(C,D) + \frac{2}{9}\sum_{m=1}^{\infty} I^c_{0,2m}(C,D)(1-4m^2)(9-4m^2)$$

$$s_2 = I^c_{0,0}(A,B) + \frac{2}{15}\sum_{m=1}^{\infty} I^c_{0,2m}(A,B)(1-4m^2)(15+4m^2)$$

$$S_2 = I^c_{0,0}(C,D) + \frac{2}{15}\sum_{m=1}^{\infty} I^c_{0,2m}(C,D)(1-4m^2)(15+4m^2).$$

References

ASME, Boiler and Pressure Vessel Code, 1977. Section XI, Rules for Inservice Inspection of Nuclear Power Plant Components.

Fu, W.S., Keer, L.N., 1969. Coplanar circular cracks under shear loading. Int. J. Engng Sci. 7, 361–373.

Kachanov, M., Laures, J.P., 1989. Three-dimensional problems of strongly interacting arbitrarily located penny-shaped cracks. International Journal of Fracture 41, 289–313.

Kassir, M.K., Sih, G.C., 1975. Three-Dimensional Crack Problems. Noordhoff, Leyden, The Netherlands.

Kostrov, B.V., Das, S., 1984. Evaluation of stress and displacement fields due to an elliptical plane shear crack. Geophys. J. Roy. Astr. Soc. 78, 19–33.

Krenk, S., 1979. A circular crack under asymmetric loads and some related integral equations. Journal of Applied Mechanics 46, 821–826.

Martin, P.A., 1986. Orthogonal polynomial solutions for elliptical cracks under shear loadings. Q. J. Mech. Appl. Math. 39, 519–534.

Nishioka, T., Atluri, S.N., 1983. Analytical solution for embedded elliptical cracks and finite element alternating method for elliptical surface cracks, subjected to arbitrary loadings. Engineering Fracture Mechanics 17, 247–268.

Roy, A., Chatterjee, M., 1992. An elliptic crack in an elastic half-space. Int. J. Engng Sci. 30, 879–890.

Roy, A., Chatterjee, M., 1994. Interaction between coplanar elliptic cracks—I Normal loading. International Journal of Solids and Structures 31, 127–144.

Segedin, C.M,. 1951. Note on a penny-shaped crack under shear. Proc. Camb. Phil. Soc. 47, 396–400.

Smith, F.W., Sorensen, D.R., 1974. The elliptical crack subjected to nonuniform shear loading. Journal of Applied Mechanics 41, 502–506.

Toor, P.M., 1975. On fracture mechanics under complex stress. Engineering Fracture Mechanics 7, 321–329.